AGU PUBLICATIONS

Geophysical Research Letters

RESEARCH LETTER
10.1002/2017GL073348

Key Points:
- Multidisciplinary monitoring framework using seismic data and space-based SO_2 measurements at African lava lake volcanoes
- Characterization of the spatiotemporal shallow magmatic activity and magma migration patterns during nearly 3 years
- New insights into the dynamics of two of the most active African volcanoes (Nyiragongo and Nyamulagira)

Supporting Information:
- Supporting Information S1
- Data Set S1
- Data Set S2
- Data Set S3
- Data Set S4
- Data Set S5
- Data Set S6
- Data Set S7
- Data Set S8
- Data Set S9
- Data Set S10

Correspondence to:
J. Barrière,
julien.barriere@ecgs.lu

Citation:
Barrière, J., A. Oth, N. Theys, N. d'Oreye, and F. Kervyn (2017), Long-term monitoring of long-period seismicity and space-based SO_2 observations at African lava lake volcanoes Nyiragongo and Nyamulagira (DR Congo), *Geophys. Res. Lett.*, *44*, doi:10.1002/2017GL073348.

Received 6 MAR 2017
Accepted 5 JUN 2017
Accepted article online 12 JUN 2017

Long-term monitoring of long-period seismicity and space-based SO_2 observations at African lava lake volcanoes Nyiragongo and Nyamulagira (DR Congo)

Julien Barrière[1,2], Adrien Oth[2], Nicolas Theys[3], Nicolas d'Oreye[1,2], and François Kervyn[4]

[1]National Museum of Natural History, Walferdange, Luxembourg, [2]European Center for Geodynamics and Seismology, Walferdange, Luxembourg, [3]Royal Belgian Institute for Space Aeronomy, Uccle, Belgium, [4]Royal Museum for Central Africa, Tervuren, Belgium

Abstract Magma ascent that may lead to an eruption is commonly accompanied by variations of long-period seismic activity and SO_2 degassing. Space-based measurements of SO_2 emission rates represent a rapidly emerging and highly convenient approach for volcano monitoring; however, combining these long-term remote sensing observations with seismic data is still rare and, in particular, the potential of such a multidisciplinary approach as volcano monitoring tool remains largely unexplored. Here shallow magmatic activity and magma migration patterns at the two closely located African volcanoes Nyiragongo and Nyamulagira are inferred from a nearly 3 years long SO_2 emissions record and seismic observations between April 2014 and February 2017. The discrimination of magma movements into shallow plumbing systems allows for signs of volcanic unrest to be deciphered on a daily time scale, even with limited instrumentation on site.

1. Introduction

Several signs of unrest commonly precede and accompany volcanic eruptions, among which gas flux and seismicity changes are of major interest. Significant SO_2 emission variations can be associated with long-period seismicity, ranging from continuous tremor [*Palma et al.*, 2008; *Zuccarello et al.*, 2013; *Conde et al.*, 2016] and long-period (LP) events (range 0.5–5 Hz) [*Jousset et al.*, 2013; *Fujiwara et al.*, 2014; *Lyons et al.*, 2016] to repetitive very long period (VLP) events (<0.5 Hz) [*Jousset et al.*, 2013; *Waite et al.*, 2013; *Zuccarello et al.*, 2013; *Dawson and Chouet*, 2014; *Kazahaya et al.*, 2015]. These seismic and degassing patterns are recognized to originate from different triggering mechanisms related to magma decompression at shallow levels, e.g., magma stiffening in the upper magma conduit leading to gas pressurization and ash-rich explosions [*Nadeau et al.*, 2011] or long-term variable degassing coupled with lava fountains and lake activity at the open vent [*Palma et al.*, 2008]. Individual LP events are often associated with shallow fluid-driven sources [*Patanè et al.*, 2008, *Chouet and Matoza*, 2013, and references therein], but they may also be generated at depth and provide information on the magma front and its migration [*Aki and Ferrazzini*, 2000]. Multidisciplinary analyses of seismicity and degassing data using seismometers and close-range UV cameras or electrochemical sensors near the summit have been shown to provide essential constraints on shallow magma transport processes [*Zuccarello et al.*, 2013; *Dawson and Chouet*, 2014; *Kazahaya et al.*, 2015]. A recent appealing remote sensing approach consists in deriving volcanic SO_2 fluxes from space-based instruments [*Carn et al.*, 2008; *Carn et al.*, 2013; *Theys et al.*, 2013], which is particularly suitable to study and monitor active volcanoes in difficult and inaccessible environments. Some recent studies provided indications for the benefit of combining space-based SO_2 measurements with seismic data in order to reveal signs of magma ascent during day-long to monthlong eruptive crises [*Jousset et al.*, 2013; *Coppola et al.*, 2015]. However, despite its prime importance in this context, the potential of such a multidisciplinary ground- and space-based approach as a continuous, long-term monitoring tool has not been investigated yet.

We apply this integrative approach between April 2014 and February 2017 to seismic and space-based SO_2 emission data from the Virunga Volcanic Province (VVP), located in the western branch of the East African Rift System and home to the volcanoes Nyiragongo and Nyamulagira (Figures 1 and S1). Nyiragongo is a stratovolcano currently hosting the largest persistent lava lake on Earth and represents a serious threat to the cities of Goma (DR Congo) and Rubavu (Rwanda), as demonstrated by two catastrophic flank eruptions in 1977 and

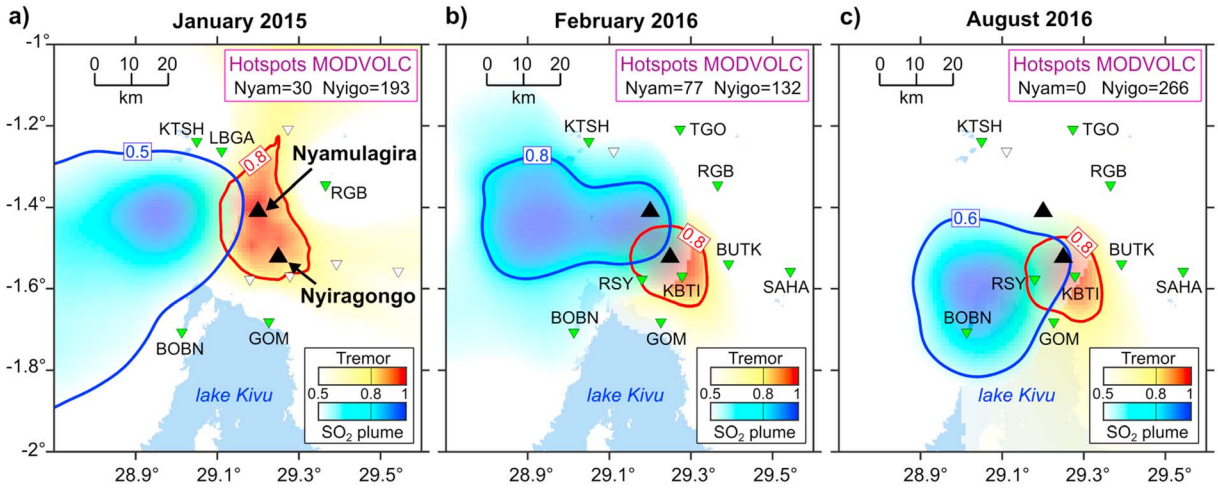

Figure 1. Location maps (1 month stack) of SO_2 plume (normalized SO_2 vertical column density retrieved from OMI) and tremor (2-D network responses) for (a) January 2015, (b) February 2016, and (c) August 2016. Available seismic stations for network response computation are depicted as green inverted triangles. SO_2 and tremor location color scales are set to the same amplitude range [0.5–1], and both data sets have been gridded onto the same 0.01° spaced geographical grid. Blue and red solid lines represent high value contours for SO_2 plume and tremor, respectively. Different contour levels between 0.5 and 0.8 are used in order to highlight the most probable source of the SO_2 plume.

2002 [*Hamaguchi et al.*, 1992; *Shuler and Ekström*, 2009; *Wauthier et al.*, 2012]. Only 13 km separate Nyiragongo from its neighbor Nyamulagira, which is a large shield volcano characterized by frequent eruptions with one eruption every 2–4 years on average [*Smets et al.*, 2010]. Following its 2011–2012 voluminous eruption, significant seismic and degassing activity persisted in the central crater leading to the resurgence of lava fountains in mid-2014 and the reappearance of a lava lake for the first time since 1938 [*Smets et al.*, 2014; *Campion*, 2014]. Only a few seismic stations have been operating sporadically in the VVP until recently [*Pagliuca et al.*, 2009], providing very limited insights into the seismic characteristics of this volcanic region [*Hamaguchi et al.*, 1992; *Shuler and Ekström*, 2009; *Mavonga et al.*, 2010; *Smets et al.*, 2015; *Wood et al.*, 2015]. The recent and progressive deployment of the broadband seismic network KivuSNet [*Oth et al.*, 2017], currently composed of 14 telemetered seismic stations within the VVP and Lake Kivu area (Figure S1 in the supporting information), opens new monitoring opportunities in this challenging environment.

2. Materials and Methods

2.1. Satellite Measurements of SO_2

SO_2 observations from the space-based Ozone Monitoring Instrument (OMI) [*Levelt et al.*, 2006], launched in 2004 on the Aura NASA platform, are used. The SO_2 vertical column density (expressed in molecules cm^{-2}), which corresponds to the integrated concentration of atmospheric SO_2 along the vertical, is retrieved from each backscattered ultraviolet spectrum of OMI based on the DOAS (Differential Optical Absorption Spectroscopy) [*Platt and Stutz*, 2008] algorithm of the Belgian Institute for Space Aeronomy (BIRA-IASB) [*Theys et al.*, 2015]. In order to obtain results that are representative of SO_2 emissions plumes in the VVP, the vertical columns are calculated for an SO_2 plume height at 4 km above sea level. A latitude-longitude box (10°S–5°N, 15–32°E) is used to monitor the daily volcanic emissions in the VVP, and no cloud filtering is applied.

To identify the dominant volcanic SO_2 source, the OMI data were gridded at 0.01° × 0.01° resolution (i.e., higher than OMI pixel size of 13 × 24 km^2) and averaged on a monthly basis (Figure 1, blue color scale). The daily total SO_2 mass for the latitude-longitude box used is estimated by converting the number of SO_2 molecules (vertical column multiplied by OMI pixel area in square centimeters) in kilotons, summed for the pixels with vertical columns $> \mu + 3\sigma$ (μ, σ being the mean and standard deviation, respectively, of daily SO_2 vertical columns retrieved over a clean Indian Ocean region). Moreover, only pixels having at least two neighboring pixels that also satisfy this criterion are selected.

2.2. Detection and Location of Continuous Seismic Tremors

The ambient seismic field has been extensively exploited in volcano seismology for the extraction of interstation Green's functions through the computation of noise cross-correlation functions (NCFs), allowing for the detection of small changes in the seismic velocity structure of the Earth's crust [*Brenguier et al*., 2008; *Brenguier et al*., 2016, and references therein].

In the VVP, we observed that NCFs in the frequency band [0.3–0.9] Hz are dominated by a highly nondiffuse noise wavefield potentially originating from a coherent tremor source (see supporting information, Text S1 and Figures S2 and S3). Recent studies have indeed shown that NCFs do not converge to the Green's functions in the case of persistent tremor but can rather be used to locate its source region [*Ballmer et al*., 2013; *Droznin et al*., 2015]. In order to confirm the existence of such persistent low-frequency tremor, we simultaneously locate its source region and determine a robust traveltime model under the simplifying assumption that the dominant tremor source is at the Earth's surface [*Ballmer et al*., 2013; *Droznin et al*., 2015]. To this end, we perform a standard grid search by reordering the NCFs according to the differential station distances with respect to every potential point source of a 2.5 km spaced 2-D grid. The best fitting traveltime curve corresponds to a global minimum associated with a source around Nyiragongo, resulting in a satisfactory fit for the whole range of differential station distances up to 90 km (Figure S4). After highlighting this continuous, low-frequency tremor source at Nyiragongo volcano, we perform a daily routine location of the dominant tremor source region by calculating the expected time lag for each 2-D grid point and each station pair using this traveltime curve. Absolute values of daily NCFs at times corresponding to the calculated delay times are stacked for all station pairs. The source location is obtained where these absolute envelope functions are coherently summed (see supporting information, Text S2). Following *Droznin et al*. [2015], this final location map is called the 2-D network response, scaled into the interval [0–1] by applying a min-max normalization (Figure 1, red color scale).

2.3. Detection and Location of Long-Period Events

Among the various approaches for locating earthquakes, a set of similar automatic techniques, which is commonly referred to as "source-scanning" algorithms [*Kao and Shan*, 2004], recently emerged as valuable location tool for events with low signal-to-noise ratio (SNR) and/or emergent onsets, both characteristics typical of volcanic environments. These methods, which mostly consist in the application of a delay-and-sum process [*Grigoli et al*., 2013, *Langet et al*., 2014] or cross correlation-based approaches [*Poiata et al*., 2016], rely on the computation of a characteristic signal time function at each single station, such as short-term/long-term average ratio [*Grigoli et al*., 2013], kurtosis [*Langet et al*., 2014], or envelope waveforms [*Poiata et al*., 2016]. Here we use a similar approach to the one employed by *Poiata et al*. [2016] based on station pair time delay estimate functions obtained by cross correlation in order to locate LP events in the frequency range 0.5–2 Hz. The principle of this interstation cross-correlation technique is similar to the tremor location procedure presented previously and is also detailed in the supporting information (see supporting information, Text S3 and Figures S5 to S6).

2.4. Template Matching for Time Periods With Limited Data Availability

Due to the progressive seismic network deployment [*Oth et al*., 2017], the limited number of available stations strongly hampered the reliable location of LP events as well as continuous tremors before October 2015 (maximum of six stations in the VVP for sporadic periods, see Figure S1). Nonetheless, stations GOM and RGB operated continuously since April 2014 with only a few data gaps and are well situated, being less than 20 km away from Nyiragongo and Nyamulagira, respectively. We therefore carry out template matching (or matched filter) procedures using records from these two seismic stations in order to retrieve the variability of long-period seismicity in the VVP since April 2014 (see section 3).

Since the full deployment of the network (i.e., October 2015), we observed a large number of LP earthquakes in the vicinity of Nyamulagira and use station RGB from April 2014 to February 2017 to systematically detect LP events with waveform envelopes similar to those of a master event that occurred beneath Nyamulagira volcano (see supporting information, Text S4 and Figure S7). We also verified that its dominant frequency content is more suggestive of an LP source process rather than path effects attenuating the high frequencies of a volcano-tectonic or volcano tectonic earthquake (see supporting information, Text S4 and Figure S8). Figure S9 displays the maximum likelihood location of the selected master LP event and the location density map of 774 events belonging to the master event's family obtained by template matching between October

2015 and February 2017. Considering a simple velocity model with essentially one interface at depths of interest (Figure S5) as well as the uncertainties associated to the station pair time delay estimates (see supporting information, Text S3 and Figure S6), the most probable source location area spreads over several kilometers, especially at depth. The common source region for these similar LP events can, however, be better constrained by stacking their individual location maps. For the full time period of available locations between October 2015 and February 2017, this results in an ellipse-like shape with the highest probability of occurrence between approximately 3 and 15 km depth (Figure S9). The depth range of these LP sources might correspond to a zone of magma storage and transfer between deep (~20 km depth) and shallow reservoirs (~4 km) [*Smets et al*., 2015; *Wauthier et al*., 2015], but the absolute depth estimate of each individual event must be interpreted with caution considering the confidence interval of the hypocenter locations. However, the relative variations of source depths within the LP cluster appear significant enough to suggest deeper fluid-driven source processes, in contrast to the observed continuous tremor at the same volcano (section 3).

In the same way, the similarity of the daily tremor signal with a chosen reference period's signal (*tremor signature)* can be quantified during times with very limited data availability by correlating the daily interstation NCFs with the NCF of the reference period [*Droznin et al*., 2015], as long as at least one suitable station pair with continuous recordings is available (see supporting information, Text S4). Finally, continuous tremor intensity variations since April 2014 can be assessed by computing standard 10 min averaged band-limited seismic amplitudes (commonly referred to as RSAM, originally defined as Real-time Seismic Amplitude Measurement) [*Endo and Murray*, 1991] at RGB station, the closest site from both volcanoes.

3. Results and Discussion

3.1. Simultaneous Location of Tremor and SO_2 Emissions

Given the OMI spatial resolution and the proximity of Nyiragongo and Nyamulagira, separating their individual contributions to the total SO_2 emission is only possible under favorable wind conditions. Figure 1 shows three maps of stacked network response (i.e., tremor) and spatial atmospheric SO_2 concentration integrated along the vertical axis estimates (i.e., SO_2 plume), each of them averaged for a month fulfilling these requirements, i.e., January 2015, February 2016, and August 2016. These time periods are all characterized by low to very low SO_2 emissions (respectively, 2.8, 0.9, and $<$0.1 kt/d on average). Despite the only six stations available in January 2015 (five in the VVP and station LWI at the south of the VVP; see Figure S1), a dominant tremor source region spreading over both Nyamulagira and Nyiragongo volcanoes is detected (Figure 1a). In contrast, the dominant tremor source in February (Figure 1b) and August 2016 (Figure 1c) are solely located close to Nyiragongo volcano. Monthly averages of the SO_2 plume density for January 2015 and August 2016 show that its main source appears to be colocated with the tremor source region. However, in February 2016, the locations of the main SO_2 plume and tremor source region at Nyamulagira and Nyiragongo, respectively, indicate that this is not always the case. The number of hot spots detected by MODVOLC, a thermal anomaly monitoring using the spatial instrument Moderate-Resolution Imaging Spectroradiometer (MODIS) [*Wright et al*., 2004], are indicated for each month. The main SO_2 plume is originating from Nyamulagira when surface activity (i.e., hot spots) is detected at this volcano (January 2015 and February 2016), while the month of August 2016 exhibits dominant SO_2 emissions at Nyiragongo (even though very low in absolute terms, less than 0.1 kt/d), and no thermal anomaly at Nyamulagira. It thus appears that Nyamulagira is the principal emitter of SO_2 as long as surface activity persists in its crater, while Nyiragongo seems to feature a stable tremor source that is not necessarily associated with the highest SO_2 emissions.

3.2. Long-Period Seismicity and SO_2 Emissions in the VVP Between April 2014 and February 2017

The template-matching methodology allows for the construction of long-term timelines of tremor signature and LP seismicity, which we combine with the total daily SO_2 mass integrated over the region from the analysis of OMI satellite spectral measurements.

Between April 2014 and February 2017, the total daily SO_2 mass emitted by both volcanoes varies over more than 3 orders of magnitude and is by far the largest (up to 130 kt/d) during lava fountaining activity and the appearance of the lava lake (up to 30 kt/d) at Nyamulagira (Figure 2a). The ensuing lava lake activity was also accompanied by sustained emissions throughout 2015, even though significantly smaller than during fountaining (a few up to 10–12 kt/d). The tremor signature shows several time intervals in 2014 and 2015 where

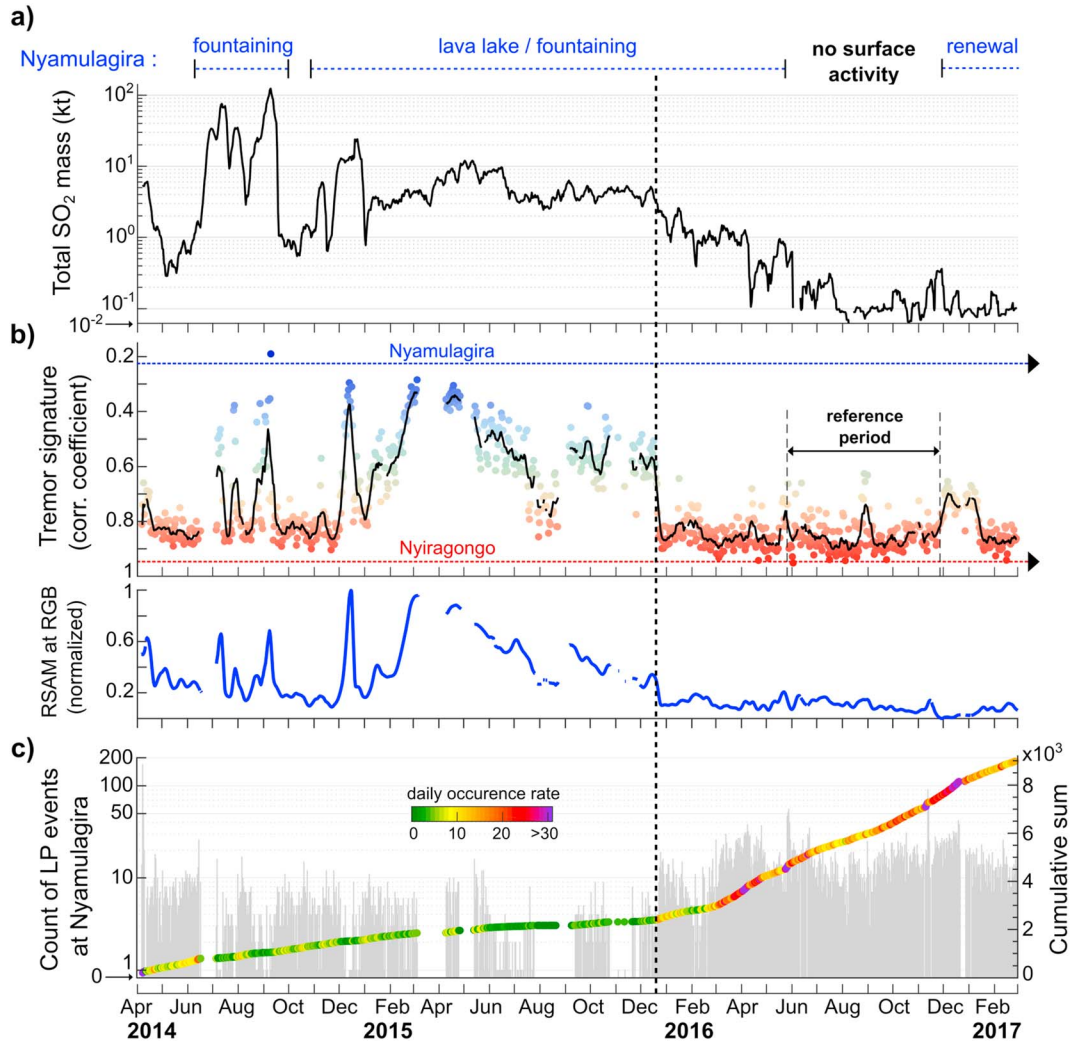

Figure 2. (a) Daily estimation of total SO_2 mass. Nyamulagira's behavior as indicated above the timeline is inferred on the basis of field observations [*Smets et al.*, 2014; GVO, personal communication, 2016] and MODVOLC thermal monitoring. (b) Normalized 10 min RSAM for stations RGB and tremor signature. For the latter, each color marker corresponds to a daily value, warm for a source at Nyiragongo and cold for Nyamulagira. (c) Daily count of LP events at Nyamulagira and corresponding cumulative sum where the color denotes the daily occurrence rate. All solid curves in this figure are smoothed with a 7 day centered moving average window (SO_2 in Figure 2a and tremor signature in Figure 2b) or a median window (RSAM in Figure 2b).

the daily NCFs are well characterized by the Nyiragongo template (Figure 2b), and in particular since early 2016 the tremor signature almost continuously depicts high correlation values (>0.8), indicating that the dominant tremor source emanates from Nyiragongo. However, the low SO_2 emissions observed in 2016 are not necessarily associated with the tremor at Nyiragongo, as shown in Figure 1 for February 2016. Intense activity at Nyamulagira in 2014 and 2015, such as vigorous lava fountaining, the birth of a lava lake [*Smets et al.*, 2014; *Campion*, 2014], and the related excess degassing, is consistently identified by low correlation values (generally lower than 0.5) in the tremor signature, indicating dominant tremor excitation at Nyamulagira coupled with degassing. Correlation values between 0.5 and 0.7 reflect a more or less pronounced contribution of both volcanoes or potential additional sources in- or outside of the VVP. The RSAM data (tremor intensity) at station RGB mimic the tremor signature with peaks during Nyamulagira tremor activity, and the lowest levels are reached in 2016 during Nyiragongo's tremor dominance.

The occurrence of LP earthquakes also exhibits strong changes during this 3 years time period (Figure 2c). In order to robustly interpret the variations in LP event occurrence rates, we first verified that the capability of

detecting the weakest events does not significantly change between periods of low or high tremor activity (see supporting information, Text S5 and Figure S10). An important LP swarm occurs at Nyamulagira at the very beginning of the data availability period (170 events on 8 April 2014). Following this short burst of activity, more moderate yet sustained LP activity carries on until the start of the fountaining activity (June 2014). During the transition from fountaining to lava lake activity, LP occurrence rates progressively decrease to their lowest level during 2015, followed by a strong, continuous increase in the number of LP events in early 2016 (Figure 2c). Two distinct behaviors of long-period seismicity (tremor and LP) and SO_2 emissions are thus clearly emphasized before and after December 2015 (dashed line). From December 2015 onward, the combination of a significant change in tremor signature toward Nyiragongo, a remarkable increase in LP activity, and a further decrease of SO_2 emissions indicate drastic changes in the dynamics of the plumbing system at Nyamulagira.

3.3. Changes in Magma Migration Patterns at Nyamulagira

Figure 3 highlights the second half of the available time period (August 2015 to March 2017) by incorporating new information displayed in Figures 3a and 3b. MODVOLC monitoring is added in order to better gauge the timing of disappearance of surface activity at Nyamulagira (Figure 3a). Figure 3b shows the depth variations of LP events detected by template matching and located with at least seven stations (see Figure S9b). Only few events are locatable before February 2016, thus not allowing any comment prior to this date.

Despite the already rather low degassing level of a few kt/d, a sudden further decrease down to the order of only 1–2 kt/day was observed on 22 December 2015 (Figure 3c). The LP activity at Nyamulagira resumed abruptly on the same day (Figure 3b). However, at the same time, the tremor signature depicts a sudden loss of the additional Nyamulagira-related signal (tremor signature between 0.5 and 0.7) and the tremor locations using all available station pairs before and after this event confirm that long-range tremor signals are not generated anymore at Nyamulagira (Figure 3d). These observations imply that the transport of fresh magma to shallow levels may have rapidly disappeared or has at least been substantially reduced. There is a transition of few months between this drop of degassing and tremor activity and the complete disappearance of the lava lake at Nyamulagira in May 2016 (Figure 3a). Between 22 December 2016 and May 2016, the remaining surface activity is accompanied by a progressive increase of LPs occurrence rate at stable depth and a continuous decrease of SO_2 emissions. As stated previously (section 2), while the absolute depth estimates of individual LP events are not very reliable, the relative variations bring crucial information about fluctuations of the magma front. Since the end of May 2016, a significant deepening of the LP source region has been accompanied by the loss of surface activity at Nyamulagira and a further marked decrease of daily SO_2 emissions down to the order of 0.1–0.2 kt (see also Figure 2). It is also worth noting that a second important swarm occurred on 25 May 2016 (Figure 3b). This period between January and May 2016 corresponds to the transition from an open conduit system characterized by shallow tremor sources and sustained SO_2 emissions to magma-driven processes at greater depth. Since this date, most of the total SO_2 emissions probably originate from Nyiragongo as illustrated in Figure 1 for August 2016. In September 2016, the LP events depth reached again a rather stable level around 10 km below sea level and was maintained until the renewal of surface activity at Nyamulagira in December 2016 (Figure 3a), which was confirmed by visual observations from the Goma Volcano Observatory team (GVO, personal communication, 2016). In November 2016, daily variations of total SO_2 mass from around 0.02 to 0.4 kt, the highest level since May 2016, could reflect the outgassing at Nyamulagira at the top of the magma column preceding the reappearance of the lava lake on 27–28 November according to MODVOLC. From this date until 1 March 2017, we have observed that the surface activity at Nyamulagira is accompanied by the same LP source depth range as in early 2016 and a sustained LP occurrence. The dominant tremor source region is still located at Nyiragongo, while SO_2 emissions remain very low in comparison to the past 3 years, thus reflecting a weak recovery of Nyamulagira activity. This contrasts to fountaining episodes in 2014 characterized by strong tremors and SO_2 emissions conveying different magma ascent and fragmentation dynamics [*Jaupart and Vergniolle*, 1988; *Parfitt and Wilson*, 1995].

3.4. Background Tremor and SO_2 Emissions Associated with the Persistent Lava Lake Activity at Nyiragongo

Nyiragongo seems to feature a continuous background tremor source, consistent with the fact that the correlation values in the tremor signature almost never drop to values below 0.2–0.3 (Figure 2b). Overall, low SO_2

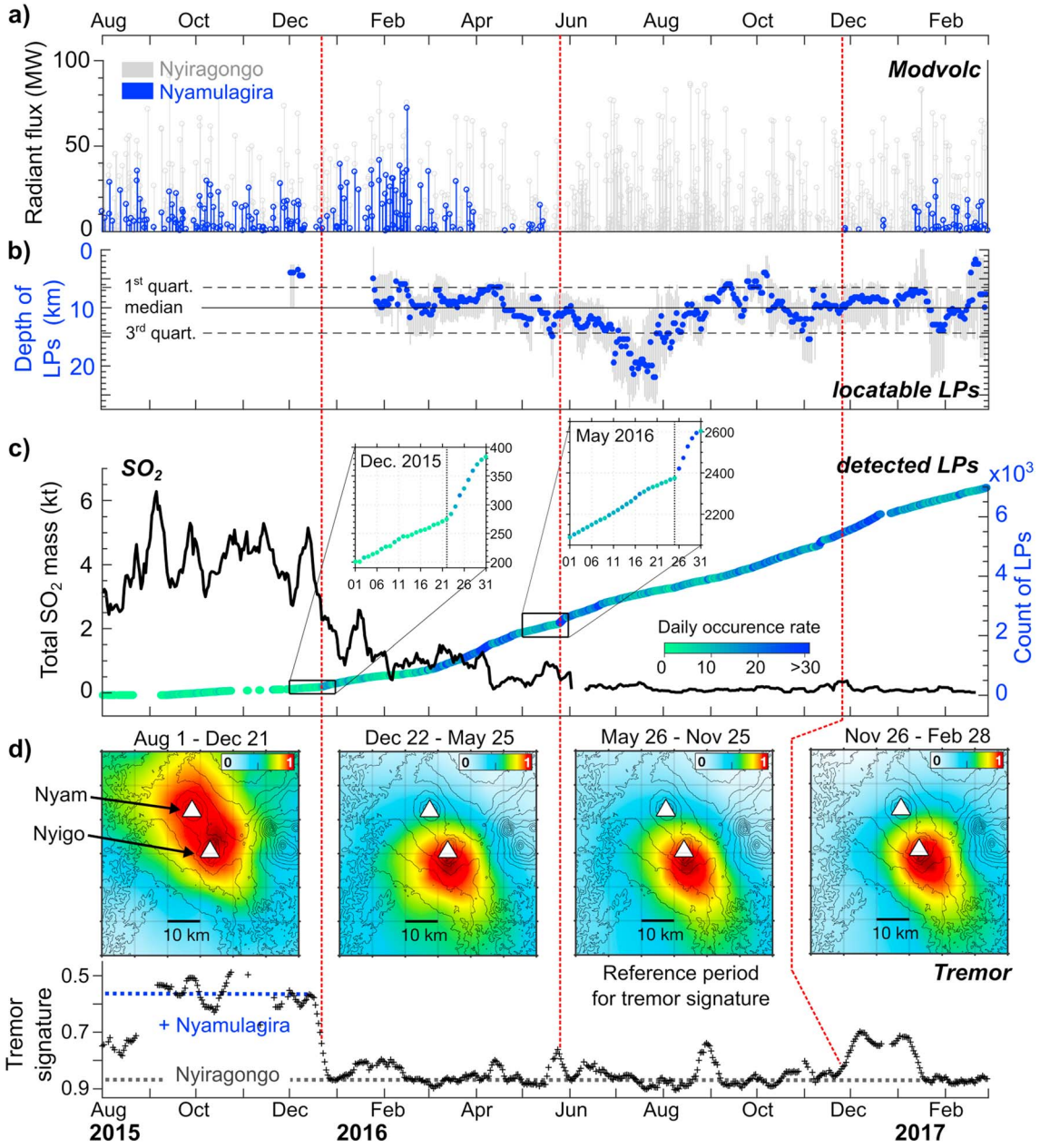

Figure 3. (a) Daily radiant flux (MW) differentiated for Nyiragongo (gray) and Nyamulagira (from MODVOLC). (b) Depths of 774 locatable LP events (Figure S9) belonging to the master event's family (i.e., detected LPs in Figure 3c). Each blue dot corresponds to the 7 day centered moving median, gray area represents 1st and 3rd quartile interval. Same statistics for the entire period are plotted as straight lines (solid and dashed). (c) Total daily SO_2 mass and count of LP events at Nyamulagira between 1 August 2015 and 1 March 2017 (zoom from Figure 2). The two insets represent the count of LP events for December 2015 and May 2016, respectively. (d) Stacked network responses (tremor location) for the four time periods separated by red dashed lines and corresponding tremor signature (zoom from Figure 2). Nyigo stands for Nyiragongo, Nyam for Nyamulagira.

emissions are associated with Nyiragongo, especially between May and November 2016 where Nyiragongo is the only volcano with surface activity in the VVP (Figures 2 and 3). Since its last eruption in 2002, characterized by very large emissions similar to levels observed at Nyamulagira during lava fountaining in 2014 (around 100 kt/d), Nyiragongo exhibits low SO_2 emission rates between few hundred to thousands of tons per day between 2004 and 2012 [*Sawyer et al.*, 2008; *Arellano et al.*, 2016]. Such low levels are in accordance with emission rates reported in this study during the disappearance of the lava lake at Nyamulagira (May–November 2016). Relatively small and stable SO_2 emissions are also common at other lava lakes [*Shinohara*, 2008], as observed for instance at Erta'Ale volcano (Ethiopia) with around 0.1 kt/day

[*Oppenheimer et al*., 2004]. Nonetheless, significant episodic behavior of the lava lake, such as gas piston activity or large bubble bursting [e.g., *Nadeau et al*., 2015], could produce distinct regimes of low and high tremor amplitudes and SO_2 emissions, as shown by *Patrick et al*. [2016] at Kilauea volcano using seismic and SO_2 degassing observations at the summit. In our study, the time resolution for tremor and SO_2 observations and the absence of close measurements to the lava lake does not allow to highlight such short-term changes. *Smets et al*. [2016] recently reported comparable variations of the lava lake at Nyiragongo, which reveal a similar behavior to gas pistoning and lava spattering at Kilauea. A large daily variability in SO_2 emission rates from Nyiragongo is also confirmed by ground-based measurements between 2004 and 2012 [*Arellano et al*., 2016]. Seismic and degassing observations obtained in this study between April 2014 and February 2017, characterized by continuous long-period tremor activity and quiescent SO_2 emissions (on a daily average), are thus most likely connected to Nyiragongo's persistent lava lake activity driven by minutes to hourly fluctuations.

Acknowledgments
This article is a contribution in the framework of the project *Remote Sensing and In Situ Detection and Tracking of Geohazards* (RESIST, http://resist.africamuseum.be), funded by the Belgian Science Policy (Belspo), Belgium, and the Fonds National de la Recherche (FNR), Luxembourg. We thank W. Thelen and S. Hurwitz for their constructive reviews, which help to improve the manuscript. We also wish to thank the Congolese Institute for Nature Preservation (ICCN) and the MONUSCO for their continuous support and for allowing us to host the stations in their compounds, as well as the entire Goma Volcano Observatory team and the sentinels of the stations, without whom the operation of the seismic network would be impossible. We thank Holger Sihler of MPIC for providing the OMI IFOV parameters and for fruitful discussions. Radiant heat flux data from MODVOLC monitoring are freely available at modis.higp.hawaii.edu. Station Bobandana (BOBN) has been installed in the framework of AfricaArray (www.africaarray.psu.edu), and its data are freely available from Incorporated Research Institutions for Seismology (IRIS) with a time delay of 3 years. All other KivuSNet data are underlying an embargo policy following the conditions of the Memoranda of Understanding between the partner institutions of RESIST. Beyond this embargo policy, data may be shared for collaboration purposes upon request with the approval of all RESIST partners. Data archiving and accessibility is ensured through the GEOFON program of the GFZ German Research Centre for Geosciences (http://dx.doi.org/doi:10.14470/XI058335), and KivuSNet is registered within the FDSN with network code KV (http://www.fdsn.org/networks/detail/KV/). Original time series presented in Figures 2 and 3 (SO_2 total mass, tremor signature, RSAM at station RGB, and LP counts) as well as the tremor/SO_2 monthly averaged location maps (Figure 1) are available as electronic supplements.

4. Conclusion

We combined the analysis of long-period seismicity with daily SO_2 emission estimates using the Ozone Monitoring Instrument (OMI) at the closely located African volcanoes Nyiragongo and Nyamulagira. Over the entire period of study (April 2014 to February 2017), Nyiragongo features a nearly constant background tremor source and low SO_2 degassing associated with the dynamics of its lava lake. In contrast, Nyamulagira exhibits a much more sporadic pattern of strong tremor associated with extensive SO_2 emissions during fountaining and lava lake activity, first observed in June 2014. The vanishing of the tremor source (most likely in the shallow edifice), the progressive decrease of SO_2 emissions, and the increase of LP events occurrence rates at greater depth convey changes of magma ascent dynamics and gas melt properties. The synergetic approach taken here allows for a robust discrimination of volcanic unrest characteristics in this complex, highly active volcanic system. Improved satellite SO_2 observations (e.g., from TROPOMI [*Veefkind et al*., 2012]) will accumulate over the years to come and further support the development of such joint ground and space-based monitoring tools for other active volcanoes worldwide. Further ground measurements (gas emissions, seismic, and infrasound), ideally close to the summits, would allow for better constraining the first insights into the volcano's internal dynamics discussed in this study.

References

Arellano, S., M. Yalire, B. Galle, N. Bobrowski, A. Dingwell, M. Johansson, and P. Norman (2016), Long-term monitoring of SO_2 quiescent degassing from Nyiragongo's lava lake, *J. Afr. Earth Sci.*, doi:10.1016/j.jafrearsci.2016.07.002, In Press.

Aki, K., and V. Ferrazzini (2000), Seismic monitoring and modeling of an active volcano for prediction, *J. Geophys. Res.*, *105*, 16,617–16,640, doi:10.1029/2000JB900033.

Ballmer, S., C. J. Wolfe, P. G. Okubo, M. M. Haney, and C. H. Thurber (2013), Ambient seismic noise interferometry in Hawai'i reveals long-range observability of volcanic tremor, *Geophys. J. Int.*, *194*, 512–523, doi:10.1093/gji/ggt112.

Bensen, G. D., M. H. Ritzwoller, M. P. Barmin, A. L. Levshin, F. Lin, M. P. Moschetti, N. M. Shapiro, and Y. Yang (2007), Processing seismic ambient noise data to obtain reliable broad-band surface wave dispersion measurements, *Geophys. J. Int.*, *169*, 1239–1260, doi:10.1111/j.1365-246X.2007.03374.x.

Brenguier, F., N. M. Shapiro, M. Campillo, V. Ferrazzini, Z. Duputel, O. Coutant, and A. Nercessian (2008), Towards forecasting volcanic eruptions using seismic noise, *Nat. Geosci.*, *1*, 126–130, doi:10.1038/ngeo104.

Brenguier, F., D. Rivet, A. Obermann, N. Nakata, P. Boué, T. Lecocq, M. Campillo, and N. Shapiro (2016), 4-D noise-based seismology at volcanoes: Ongoing efforts and perspectives, *J. Volcanol. Geotherm. Res.*, *321*, 182–195, doi:10.1016/j.jvolgeores.2016.04.036.

Campion, R. (2014), New lava lake at Nyamuragira volcano revealed by combined ASTER and OMI SO_2 measurements, *Geophys. Res. Lett.*, *41*, 7485–7492, doi:10.1002/2014GL061808.

Carn, S. A., A. J. Krueger, S. Arellano, N. A. Krotkov, and K. Yang (2008), Daily monitoring of Ecuadorian volcanic degassing from space, *J. Volcanol. Geotherm. Res.*, *176*, 141–150, doi:10.1016/j.jvolgeores.2008.01.029.

Carn, S. A., N. A. Krotkov, K. Yang, and A. J. Krueger (2013), Measuring global volcanic degassing with the Ozone Monitoring Instrument (OMI), *Geol. Soc. London, Spec. Publ.*, *380*, 229–257, doi:10.1144/SP380.12.

Chouet, B. A., and R. S. Matoza (2013), A multi-decadal view of seismic methods for detecting precursors of magma movement and eruption, *J. Volcanol. Geotherm. Res.*, *252*, 108–175, doi:10.1016/j.jvolgeores.2012.11.013.

Conde, V., S. Bredemeyer, J. A. Saballos, B. Galle, and T. H. Hansteen (2016), Linking SO_2 emission rates and seismicity by continuous wavelet transform: Implications for volcanic surveillance at San Cristóbal volcano, Nicaragua, *Int. J. Earth Sci.*, *105*, 1453–1465, doi:10.1007/s00531-015-1264-1.

Coppola, D., et al. (2015), Magma extrusion during the Ubinas 2013–2014 eruptive crisis based on satellite thermal imaging (MIROVA) and ground-based monitoring, *J. Volcanol. Geotherm. Res.*, *302*, 199–210, doi:10.1016/j.jvolgeores.2015.07.005.

Dawson, P., and B. A. Chouet (2014), Characterization of very-long-period seismicity accompanying summit activity at Kilauea volcano, Hawai'i: 2007–2013, *J. Volcanol. Geotherm. Res.*, *278*, 59–85, doi:10.1016/j.jvolgeores.2014.04.010.

Droznin, D. V., N. M. Shapiro, S. Y. Droznina, S. L. Senyukov, V. N. Chebrov, and E. I. Gordeev (2015), Detecting and locating volcanic tremors on the Klyuchevskoy group of volcanoes (Kamchatka) based on correlations of continuous seismic records, *Geophys. J. Int.*, *203*, 1001–1010, doi:10.1093/gji/ggv342.

Endo, E. T., and T. Murray (1991), Real-Time seismic Amplitude Measurement (RSAM): A volcano monitoring and prediction tool, *Bull. Volcanol.*, *53*, 533–545, doi:10.1007/BF00298154.

Fujiwara, Y., H. Yamasato, T. Shimbori, and T. Sakai (2014), Characteristics of dilatational infrasonic pulses accompanying low-frequency earthquakes at Miyakejima volcano, Japan, *Earth Planets Space*, *66*(11), doi:10.1186/1880-5981-66-11.

Grigoli, F., S. Cesca, M. Vassalo, and T. Dahm (2013), Automated seismic event location by travel-time stacking: An application to mining induced seismicity, *Seismol. Res. Lett.*, *84*, 666–677, doi:10.1785/0220120191.

Hamaguchi, H., T. Nishimura, and N. Zana (1992), Process of the 1977 Nyiragongo eruption inferred from the analysis of long-period earthquakes and volcanic tremors, *Tectonophysics*, *209*, 241–254, doi:10.1016/0040-1951(92)90028-5.

Jaupart, C., and S. Vergniolle (1988), Laboratory models of Hawaiian and Strombolian eruptions, *Nature*, *331*, 58–60, doi:10.1038/331058a0.

Jousset, P., A. Budi-Santoso, A. D. Jolly, M. Boichu, S. D. Surono, S. Sumarti, S. Hidayati, and P. Thierry (2013), Signs of magma ascent in LP and VLP seismic events and link to degassing: An example from the 2010 explosive eruption at Merapi volcano, Indonesia, *J. Volcanol. Geotherm. Res.*, *261*, 171–192, doi:10.1016/j.jvolgeores.2013.03.014.

Kao, H., and S. J. Shan (2004), The source-scanning algorithm: Mapping the distribution of seismic sources in time and space, *Geophys. J. Int.*, *157*, 589–594, doi:10.1111/j.1365-246X.2004.02276.x.

Kazahaya, R., Y. Maeda, T. Mori, H. Shinohara, and M. Takeo (2015), Changes to the volcanic outgassing mechanism and very-long-period seismicity from 2007 to 2011 at Mt. Asama, Japan, *Earth Planet. Sci. Lett.*, *418*, 1–10, doi:10.1016/j.epsl.2015.02.034.

Langet, N., A. Maggi, A. Michelini, and F. Brenguier (2014), Continuous kurtosis-based migration for seismic event detection and location, with application to Piton de la Fournaise volcano, La Réunion, *Bull. Seismol. Soc. Am.*, *104*, 229–246, doi:10.1785/0120130107.

Levelt, P. F., G. H. J. van den Oord, M. R. Dobber, A. Mälkki, H. Visser, J. de Vries, P. Stammes, J. Lundell, and H. Saari (2006), The Ozone Monitoring Instrument, *IEEE Trans. Geotherm. Remote Sens.*, *44*(5), 1093–1101, doi:10.1109/TGRS.2006.872333.

Lomax, A., A. Michelini, and A. Curtis (2009), Earthquake location, direct, global-search methods, in *Complexity in Encyclopedia of Complexity and System Science*, pp. 2449–2473, Springer, New York.

Lyons, J. J., M. M. Haney, C. Werner, P. Kelly, M. Patrick, C. Kern, and F. Trusdell (2016), Long period seismicity and very long period infrasound driven by shallow magmatic degassing at Mount Pagan, Mariana Islands, *J. Geophys. Res. Solid Earth*, *121*, 188–209, doi:10.1002/2015JB012490.

Mavonga, T., N. Zana, and R. J. Durrheim (2010), Studies of crustal structure, seismic precursors to volcanic eruptions and earthquake hazard in the eastern provinces of the Democratic Republic of Congo, *J. Afr. Earth Sci.*, *58*, 623–633, doi:10.1016/j.jafrearsci.2010.08.008.

Nadeau, P. A., J. L. Palma, and G. P. Waite (2011), Linking volcanic tremor, degassing, and eruption dynamics via SO_2 imaging, *Geophys. Res. Lett.*, *38*, L01304, doi:10.1029/2010GL045820.

Nadeau, P. A., C. A. Werner, G. P. Waite, S. A. Carn, I. D. Brewer, T. Elias, A. J. Sutton, and C. Kern (2015), Using SO_2 camera imagery and seismicity to examine degassing and gas accumulation at Kīlauea volcano, May 2010, *J. Volcanol. Geotherm. Res.*, *300*, 70–80, doi:10.1016/j.jvolgeores.2014.12.005.

Oppenheimer, C., A. J. S. McGonigle, P. Allard, M. J. Wooster, and V. Tsanev (2004), Sulfur, heat, and magma budget of Erta'Ale lava lake, Ethiopia, *Geology*, *32*, 509–512, doi:10.1130/G20281.1.

Oth, A., et al. (2017), KivuSNet: The first dense broadband seismic network for the Kivu Rift region (western branch of East African Rift), *Seismol. Res. Lett.*, *88*(1), 49–60, doi:10.1785/0220160147.

Palma, J. L., E. S. Calder, D. Basualto, S. Blake, and D. A. Rothery (2008), Correlations between SO_2 flux, seismicity, and outgassing activity at the open vent of Villarrica volcano, Chile, *J. Geophys. Res.*, *113*, B10201, doi:10.1029/2008JB005577.

Pagliuca, N. M., et al. (2009), Preliminary results from seismic monitoring at Nyiragongo volcano (Democratic Republic of Congo) through telemetered seismic network, Goma Volcanological Observatory, *Bull. di Geof. Teor. ed Appl.*, *50*, 117–127.

Parfitt, E. A., and L. Wilson (1995), Explosive volcanic eruptions: IX. The transition between Hawaiian-style lava fountaining and Strombolian explosive activity, *Geophys. J. Int.*, *121*, 226–232, doi:10.1111/j.1365-246X.1995.tb03523.x.

Patanè, D., G. Di Grazia, A. Cannata, P. Montalto, and E. Boschi (2008), Shallow magma pathway geometry at Mt. Etna volcano, *Geochem. Geophys. Geosyst.*, *9*, Q12021, doi:10.1029/2008GC002131.

Patrick, M. R., T. Orr, A. J. Sutton, E. Lev, W. Thelen, and D. Fee (2016), Shallowly driven fluctuations in lava lake outgassing (gas pistoning), Kilauea volcano, *Earth Planet. Sci. Lett.*, *433*, 326–338.

Platt, U., and J. Stutz (2008), *Differential Optical Absorption Spectroscopy (DOAS), Principle and Applications*, Springer, Heidelberg.

Podvin, P., and I. Lecomte (1991), Finite difference computation of traveltimes in very contrasted velocity models: A massively parallel approach and its associated tools, *Geophys. J. Int.*, *105*, 271–284, doi:10.1111/j.1365-246X.1991.tb03461.x.

Poiata, N. C. S., J. P. Vilotte, P. Bernard, and K. Obara (2016), Multiband array detection and location of seismic sources recorded by dense seismic networks, *Geophys. J. Int.*, *205*, 1548–1573, doi:10.1093/gji/ggw071.

Sawyer, G. M., S. A. Carn, V. I. Tsanev, C. Oppenheimer, and M. Burton (2008), Investigation into magma degassing at Nyiragongo volcano, Democratic Republic of the Congo, *Geochem. Geophys. Geosyst.*, *9*, Q02017, doi:10.1029/2007GC001829.

Shinohara, H. (2008), Excess degassing from volcanoes and its role on eruptive and intrusive activity, *Rev. Geophys.*, *46*, RG4005, doi:10.1029/2007RG000244.

Shuler, A., and G. J. Ekström (2009), Anomalous earthquakes associated with Nyiragongo volcano: Observations and potential mechanisms, *J. Volcanol. Geotherm. Res.*, *181*, 219–230, doi:10.1016/j.jvolgeores.2009.01.011.

Smets, B., C. Wauthier, and N. D'Oreye (2010), A new map of the lava flow field of Nyamulagira (D.R. Congo) from satellite imagery, *J. Afr. Earth Sci.*, *58*, 778–786, doi:10.1016/j.jafrearsci.2010.07.005.

Smets, B., N. D'Oreye, and F. Kervyn (2014), Toward another lava lake in the Virunga volcanic field?, *Eos Trans. AGU*, *95*, 377–378.

Smets, B., F. Kervyn, N. D'Oreye, and M. Kervyn (2015), Spatio-temporal dynamics of eruptions in a youthful extensional setting: Insights from Nyamulagira volcano (D.R. Congo), in the western branch of the East African Rift, *Earth Sci. Rev.*, *150*, 305–328, doi:10.1016/j.earscirev.2015.08.008.

Smets, B., N. D'Oreye, M. Kervyn, and F. Kervyn (2016), Gas piston activity of the Nyiragongo lava lake: First insights from a stereographic time-lapse camera system, *J. Afr. Earth Sci.*, doi:10.1016/j.jafrearsci.2016.04.010, in Press.

Theys, N., et al. (2013), Volcanic SO_2 fluxes derived from satellite data: A survey using OMI, GOME-2, IASI and MODIS, *Atmos. Chem. Phys.*, *13*, 5945–5968, doi:10.5194/acp-13-5945-2013.

Theys, N., et al. (2015), Sulfur dioxide vertical column DOAS retrievals from the Ozone Monitoring Instrument: Global observations and comparison to ground-based and satellite data, *J. Geophys. Res. Atmos.*, *120*, 2470–2491, doi:10.1002/2014JD022657.

Veefkind, J. P., et al. (2012), TROPOMI on the ESA Sentinel-5 Precursor: A GMES mission for global observations of the atmospheric composition for climate, air quality and ozone layer applications, *Remote Sens. Environ.*, *120*, 70–83, doi:10.1016/j.rse.2011.09.027.

Waite, G. P., P. A. Nadeau, and J. J. Lyons (2013), Variability in eruption style and associated very long period events at Fuego volcano, Guatemala, *J. Geophys. Res. Solid Earth*, *118*, 1526–1533, doi:10.1002/jgrb.50075.

Wauthier, C., V. Cayol, F. Kervyn, and N. d'Oreye (2012), Magma sources involved in the 2002 Nyiragongo eruption, as inferred from an InSAR analysis, *J. Geophys. Res.*, *117*, B05411, doi:10.1029/2011JB008257.

Wauthier, C., V. Cayol, B. Smets, N. d'Oreye, and F. Kervyn (2015), Magma pathways and their interactions inferred from InSAR and stress modeling at Nyamulagira volcano, D.R. Congo, *Remote Sens.*, *7*, 15179–15202, doi:10.3390/rs71115179.

Wright, R., L. P. Flynn, H. Garbeil, A. J. L. Harris, and E. J. Pilger (2004), MODVOLC: Near-real-time thermal monitoring of global volcanism, *J. Volcanol. Geotherm. Res.*, *135*, 29–49, doi:10.1016/j.jvolgeores.2003.12.008.

Wood, D. A., H. J. Zal, C. A. Scholz, C. J. Ebinger, and I. Nizere (2015), Evolution of the Kivu Rift, East Africa: Interplay among tectonics, sedimentation and magmatism, *Basin Res.*, *29*(S1), 175–188, doi:10.1111/bre.12143.

Zuccarello, L., M. R. Burton, G. Saccorotti, C. J. Bean, and D. Patanè (2013), The coupling between very long period seismic events, volcanic tremor, and degassing rates at Mount Etna volcano, *J. Geophys. Res. Solid Earth*, *118*, 4910–4921, doi:10.1002/jgrb.50363.